Research article

Journal of PeptideScience

Received: 29 July 2015 Revised: 7 September 2015 Accepted: 14 September 2015 Published online in Wiley Online Library

(wileyonlinelibrary.com) DOI 10.1002/psc.2828

Fullerene-based inhibitors of HIV-1 protease

T. Amanda Strom,[a] Serdar Durdagi,[b,c] Suha Salih Ersoz,[d] Ramin Ekhteiari Salmas,[b] Claudiu T. Supuran[e] and Andrew R. Barron[a,f,g]*

A series of Fmoc-Phe(4-aza-C_{60})-OH of fullerene amino acid derived peptides have been prepared by solid phase peptide synthesis, in which the terminal amino acid, Phe(4-aza-C_{60})-OH, is derived from the dipolar addition to C_{60} of the Fmoc-Nα-protected azido amino acids derived from phenylalanine: Fmoc-Phe(4-aza-C_{60})-Lys_3-OH (1), Fmoc-Phe(4-aza-C_{60})-Pro-Hyp-Lys-OH (2), and Fmoc-Phe(4-aza-C_{60})-Hyp-Hyp-Lys-OH (3). The inhibition constant of our fullerene aspartic protease PRIs utilized FRET-based assay to evaluate the enzyme kinetics of HIV-1 PR at various concentrations of inhibitors. Simulation of the docking of the peptide Fmoc-Phe-Pro-Hyp-Lys-OH overestimated the inhibition, while the amino acid PRIs were well estimated. The experimental results show that C_{60}-based amino acids are a good base structure in the design of protease inhibitors and that their inhibition can be improved upon by the addition of designer peptide sequences.

Keywords: HIV-1; fullerene; C_{60}; inhibitor; solid phase peptide synthesis; computation

Introduction

When a person is infected with HIV the virus encodes for several enzymes, including RT, integrase, and PR. The first two enzymes are responsible for transcribing and integrating the virus's genetic material into that of the host's, thereby hijacking the host's cells to produce viral proteins. HIV-1 PR is one of the viral proteins produced. It is an aspartic protease (Asp PR) [1] responsible for catalyzing the hydrolysis of precursor polyproteins associated with HIV infection [2,3]. Without the function of either RT or PR, the virus fails to mature and does not become infectious; consequently, both, RT and PR have become popular targets for HIV inhibition [4,5].

The structures of Asp PRs are somewhat variable with about 5% of the structure conserved between all strains [1]. Functional retroviral Asp PRs form a homodimer [6,7], with two identical monomers each contributing a highly conserved region near the catalytic aspartic acids. The highly conserved region consists of a triad of residues, Asp-Thr-Gly, and other hydrophobic residues, such as alanine and phenylalanine [8]. In addition to the aspartyl residues, the dimerized enzyme contains a binding pocket made up of various hydrophobic amino acids. This forms the active site of HIV-1 PR and is the region where mutations often occur in response to specific interactions with inhibitors [2]. The active site is covered over by one or two binding loops or flaps, depending on whether they are cellular or retroviral PRs, respectively, which take part in binding to substrates and inhibitors. In a general acid–base mechanism, the nucleophilic aspartyl residue initiates peptide hydrolysis by deprotonating a coordinated water molecule, or thiol in some cases, thereby generating a nucleophile capable of cleaving the amide bond [9,10]. The determination of the structure and potential mechanism of Asp PRs was a result of the initial sequencing and crystal structure of pepsin, the digestive enzyme [11], and through co-crystallization of various Asp PRs with the inhibitor pepstatin [6]. As a result researchers were able to design several classes of new inhibitors based on a remarkably accurate model of the binding pocket and its relevant interactions with inhibitors. Of primary importance were the following: (i) displacement of the nucleophilic water molecule; (ii) hydrogen bonding between the enzyme and the peptide backbone of pepstatin; (3) van der Waals interactions between the side chains of pepstatin and enzyme residues, usually hydrophobic; and (4) a conformational change in the flap of the enzyme allowing more favorable hydrogen bonding opportunities with pepstatin [5]. Through the combined efforts of many researchers, several classes of aspartic PRIs emerged.

* *Correspondence to: Prof. A. R. Barron. Department of Chemistry, Rice University, 6100 Main Street, Houston, TX 77005, USA. E-mail: arb@rice.edu*

a *Department of Chemistry, Rice University, Houston, TX 77005, USA*

b *Department of Biophysics, School of Medicine, Bahcesehir University, Istanbul, Turkey*

c *Department of Biological Sciences, Institute for Biocomplexity and Informatics, University of Calgary, Calgary, Alberta, Canada*

d *School of Medicine, Bahcesehir University, Istanbul, Turkey*

e *Laboratorio di Chimica Bioinorganica, Università degli Studi di Firenze, Rm. 188, Via della Lastruccia 3, I-50019, Sesto Fiorentino (Firenze), Italy*

f *Department of Materials Science and Nanoengineering, Rice University, Houston, TX 77005, USA*

g *Institute of Life Sciences, Swansea University, Singleton Park, Swansea SA2 8PP, Wales, UK*

Abbreviations: *Baa, 'bucky amino acid' [60]fullerene-substituted phenylalanine; Boc, di-tert-butyl dicarbonate; DCM, dichloromethane; DIEA, diisopropylethylamine; DMF, dimethylformamide; DMSO, dimethyl sulfoxide; Et_2O, diethyl ether; Fmoc, 9-fluorenylmethoxycarbonyl; FRET, fluorescence resonance energy transfer; HOBt, 1-hydroxy-1,2,3-benzotriazole; HPLC, high performance liquid chromatography; MALDI, matrix-assisted laser desorption ionization; MeCN, acetonitrile; MeOH, methanol; PR, protease; PRI, protease inhibitor; PyBop, benzotriazol-1-yl-oxytripyrrolidinophosphonium hexafluorophosphate; RT, reverse transcriptase.*

Journal of PeptideScience

Since the first known inhibitor of HIV-1 PR, pepstatin A (Figure 1), and the substrate are both peptides, most early inhibitors were either peptides or were designed as substrate mimics. One observation made from these early studies was that HIV-1 PR was able to recognize and cleave the Tyr-Pro or Phe-Pro dipeptide sequences of viral polyproteins, unlike cellular proteases, and it was correctly thought that this condition imparts some level of specificity for HIV-1 PR [12].

Based on the previous studies, a new series of peptidomimetic inhibitors were designed to imitate the tetrahedral transition state of the enzyme catalyzed reaction. Several structures were considered to emulate the proteolytic transition state of the Tyr-Pro or Phe-Pro dipeptide structure; the most successful of which was a nonhydrolyzable hydroxyethylamine subunit [2]. In fact, the majority of currently available, FDA approved, inhibitors use a nonhydrolyzable hydroxyethylene or hydroxyethylamine subunit at the core [13,14]. In addition to the specificity for the dipeptide sequence, it was also discovered that an R stereo-configuration at the central carbon bearing the hydroxyl group was preferred for short PRIs [15]. The effectiveness of PR inhibitors has been diminished by the virus's high rate of mutation forcing patients to take 'cocktails' of drugs to combat the constantly changing virus. The need for structurally novel inhibitors of HIV-1 PR is evident.

In an effort to find new and potent inhibitors of HIV-1 PR, many molecules have been considered. The fit of C_{60} with the binding pocket of HIV-1 PR was first proposed by Friedman in 1993, when he realized that C_{60} would actually make quite a nice fit, both through steric and electrostatic interactions [16]. Since Friedman's initial work many others have attempted to improve the affinity of fullerene derivatives for the active site of HIV-1 PR [17–19]. Despite many attempts by several researchers to make potent, water-soluble, fullerene PRI, the most potent of the fullerene inhibitors was designed by modeling hydrophobic de-solvation upon complex formation with PR [20].

We have previously investigated the inhibition activity of various fullerene amino acids [21], and this has led to an interest in whether the combination of the fit of C_{60} with the binding pocket of HIV-1 PR with the structural attributes of current peptidomimetic inhibitors will provide added inhibition activity over the component derivatives. Fullero-peptides utilizing an unnatural C_{60} amino acid were first reported by Prato and co-workers [22], who recognized the novel properties a fullerene might impart to biological molecules. Since that time our laboratory has produced several fullerene amino acids [23–25] and peptide derivatives [26,27] to investigate their cellular penetrating properties [28,29], their transport through skin [30], their inhibition of neuroblastoma [26], and their ability to inhibit carbonic anhydrase [31]. Others have investigated the cytotoxicity, DNA cleavage, and enzyme inhibition by fullerene amino acids, peptides, and other C_{60} derivatives [32–38].

In our current investigation of fullerene inhibitors of HIV-1 PR we wanted to answer several questions: (i) will a fullerene amino acid be a good base for the design of fullerene-based PRIs, (ii) will subtle changes to the C_{60} amino acid core affect the achieved inhibition, and (iii) can we improve the inhibition of the fullerene amino acid through the incorporation of a designer peptide tail? Given that the synthesis and purification of fullerene compounds can be time-consuming and expensive, the use of molecular docking simulations aided us in the discovery of lead compounds and in the design of new inhibitors [21,39].

Materials and methods

Fmoc-Phe(4-aza-C_{60})-OH and the other fullerene amino acids were prepared by previously reported methods [23–25]. The FRET peptide substrate, HIV-1 PR, and assay buffer A (Tris, glycerol, KCl, DTT, and EDTA with 500 mM KCl, pH 4.7) were provided in the ProAssay™ HIV-Protease kit from ProteinOne. The peptide sequence of the FRET peptide substrate is derived from the native p17/p24 cleavage site on Prgag (native substrate) for HIV-1 protease. Protected amino acids were purchased from Chem-Impex International, Inc., unless otherwise specified, and used without further purification. All inhibitor peptide sequences were purchased from BioSynthesis, Inc. in the crude form on Wang resin. HOBt, TFA, TIPS, DCM, DIEA, DMF, PyBop, DMSO and all solvents were purchased from Sigma Aldrich and used without further purification. All other chemicals and reagents were purchased from Sigma-Aldrich. HPLC was performed on a Varian ProStar instrument using a Varian Dynamax C_{18} column (250 × 21.6 mm) for purification when necessary. Mass spectrometry measurements were performed on a Bruker AutoFlex II/ToF/ToF and a Bruker Electrospray Ionization/μToF. α-Cyano-4-hydroxycinnamic acid was used as the matrix to characterize all peptides by MALDI/TOF (positive mode). UV-visible spectra were recorded on a Varian Cary 5000 spectrometer. Fluorescence data were recorded on a BioTek Synergy 4 fluorescence plate reader.

General fullerene peptide synthesis

All peptides were purchased on the resin with orthogonal protection for Fmoc SPPS on the side chains and N-terminus. The fullerene amino acid, or a control amino acid, was coupled to the peptide sequence through published literature methods in a 3 : 1 amino acid to peptide ratio [40]. The reaction mixture was shielded from light throughout the synthesis and purification. Peptides were cleaved from the resin using 20% TFA with 2.5% TIPS in DCM and precipitated with cold diethyl ether then washed with ether (3 × 50 ml). The crude peptide was dissolved in an appropriate solvent or buffer and mixed with a small amount of C_{18} coated silica gel and immediately filtered to remove the salts for analysis then lyophilized and stored under vacuum in the dark. When necessary the peptide was purified by HPLC (C_{18} prep scale, 95 : 5–5 : 95 0.1% formic acid and isopropanol, 65 min). The major impurity present is C_{60} by ESI MS.

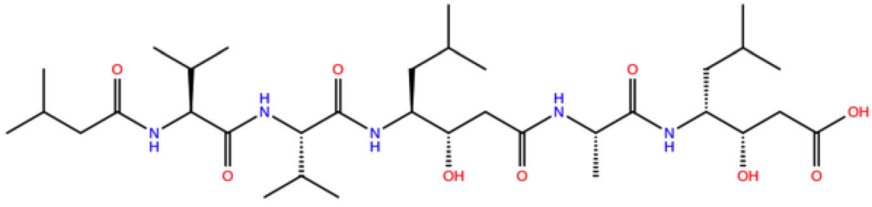

Figure 1. The chemical structure of pepstatin A.

Fmoc-Phe(4-aza-C_{60})-Lys_3-OH (1)

The crude peptide, Fmoc-Lys(Boc)-[Lys(Boc)]$_2$-Wang resin (215.5 mg, 0.2 mmol/g_{resin}), was added to a 10 ml SPPS synthesis vessel. DMF was used to swell the resin for 1 h then filtered. The Fmoc protecting group on the terminal Lys residue was removed with 25% piperidine in DMF (2 × 10 ml) after which the resin was rinsed with DMF (3 × 10 ml). Fmoc-Phe(4-N-aza-C_{60})-OMe (150 mg, 0.132 mmol), HOBt (17.81 mg, 0.132 mmol), PyBop (68.64 mg, 0.132 mmol), and DIEA (68.9 µl, 0.396 mmol) were dissolved in DMF : DCM (1 : 2, 8 ml) and sonicated for 2 min then added to the resin. The synthesis vessel was always kept in the dark, and the reaction was mixed for 24 h. The excess reagents were filtered away, and the resin was washed with DCM (3 × 10 ml), and DMF (3 × 10 ml) then the resin was shrunk with MeOH (3 × 10 ml). The peptide was cleaved from the resin with 20:2.5:77.5 TFA:TIPS:DCM and precipitated and washed with the addition of cold Et_2O (3 × 50 ml). ESI/TOF shows the major impurity is C_{60}. To remove C_{60} the peptide is dissolved in DMSO and filtered through a C_{18} silica plug. The product was lyophilized to dryness. Yield: 33 mg, 50%. ESI/TOF (M+1) requires *m/z* 1505.43, found *m/z* 1505.45.

Fmoc-Phe(4-aza-C_{60})-Pro-Hyp-Lys-OH (2)

The crude peptide, Fmoc-Pro-Hyp(tBu)-Lys(Boc)-Wang resin (102.63, 0.217 mmol/g_{resin}, 0.022 mmol), was added to a 10 ml SPPS synthesis vessel. DMF was used to swell the resin for 1 h then filtered. The Fmoc protecting group on the terminal Lys residue was removed with 25% piperidine in DMF (2 × 10 ml) after which the resin was rinsed with DMF (3 × 10 ml). Fmoc-Phe(4-N-aza-C_{60})-OMe (75 mg, 0.067 mmol), HOBt (9.04 mg, 0.067 mmol), PyBop (34.83 mg, 0.067 mmol), and diisopropylethylamine (DIEA, 35 µl, 0.201 mmol) were dissolved in DMF : DCM (1 : 2, 8 ml) and sonicated for 2 min then added to the resin. The synthesis vessel was always kept in the dark, and the reaction was mixed for 24 h. The excess reagents were filtered away and the resin was washed with DCM (3 × 10 ml), and DMF (3 × 10 ml) then the resin was shrunk with MeOH (3 × 10 ml). The peptide was cleaved from the resin with 20:2.5:77.5 TFA : TIPS : DCM and precipitated and washed with the addition of cold Et_2O (3 × 50 ml). The peptide was pure as cleaved off the resin by ESI/ToF with a minor C_{60} impurity. The product was dissolved in MeCN : H_2O (1 : 1, 1.0 ml) and lyophilized to dryness. Yield: 53 mg, 80%. ESI/TOF (M + 1) requires *m/z* 1459.41, found *m/z* 1459.34.

Fmoc-Phe(4-aza-C_{60})-Hyp-Hyp-Lys-OH (3)

Prepared in a similar manner to compound **2** using the crude peptide, Fmoc-Hyp(tBu)-Hyp(tBu)-Lys(Boc)-Wang resin (100.40 mg, 0.22 mmol/g_{resin}, 0.022 mmol), Fmoc-Phe(4-N-aza-C_{60})-OMe (75 mg, 0.067 mmol), HOBt (9.04 mg, 0.067 mmol), PyBop (34.83 mg, 0.067 mmol), and DIEA (35 µl, 0.201 mmol). Yield: 27.6 mg, 85%. ESI/TOF (M+1) requires *m/z* 1475.90, found *m/z* 1476.23.

Stearoyl-Lys_3-OH (4)

Prepared in a similar manner to compound **1** using the crude peptide, Fmoc-Lys(Boc)-[Lys(Boc)]$_2$-Wang resin (74.88 mg, 0.266 mmol/g_{resin}, 0.02 mmol), stearic acid (17 mg, 0.06 mmol), HOBt (8.07 mg, 0.06 mmol), PyBop (31.10 mg, 0.06 mmol), and DIEA (31.2 µl, 0.179 mmol). Yield: 12.05 mg, 90%. ESI/TOF (M + 1) requires *m/z* 669.56, found *m/z* 669.54.

Fmoc-Phe(4-NH_2)-Pro-Hyp-Lys-OH (5)

Prepared in a similar manner to compound **2** using the crude peptide, Fmoc-Pro-Hyp(tBu)-Lys(Boc)-Wang resin (71.6 mg, 0.22 mmol/g_{resin}), Fmoc-Phe(4-NH_2)-OH (20.0 mg, 0.047 mmol), HOBt (6.3 mg, 0.047 mmol), PyBop (24.3 mg, 0.047 mmol), and DIEA (24.4 µl, 0.140 mmol) Yield: 11 mg, 90%. ESI/TOF (M + 1) requires *m/z* 767.91, found *m/z* 767.34.

Determination of substrate K_m

The K_m of a substrate is determined by evaluating the initial velocity of substrate hydrolysis at various substrate concentrations in the absence of an inhibitor. The concentrations of substrate assayed by this method were from 16.5–0.2 µM. Substrate hydrolysis was followed as an increase in fluorescence (excitation/emission 490/530 nm). Data were collected at 25 °C for 1 h, or as long as the data remained linear, at 1 min increments. The total reaction volume was 25 µl. The kinetic parameters K_m and V_{max} were determined by fitting the reaction progress curve to the Michaelis–Menten (M-M) equation [41]. Figure 2 shows the M-M plot of our enzyme kinetic data with HIV-1 PR (red curve). All data presented were the average of at least duplicate measurements. The K_m of our substrate was determined to be 0.6 µM. All further kinetic inhibition assays were performed at a substrate concentration of ~1 µM. We confirmed that our enzyme was following M-M kinetics by fitting the data to the equation for a standard rectangular hyperbola (Figure 2, green curve).

Determination of total active site concentration [E_t]

The total active site concentration values were determined by a cell-free FRET based assay. Typically, 1 pmol (12 µl, 0.09 µM) of HIV-1 PR was added to 13 µl of dilution buffer A containing the substrate at a concentration near its K_m (1 µM) and various concentrations of a tight binding inhibitor dissolved in DMSO (final concentrations from 100 µM to 0.01 nM). The final concentrations of DMSO were kept below 2.5% (v/v). Substrate hydrolysis was followed as an increase in fluorescence (excitation/emission 490/530 nm). Data were collected at 25 °C for 1 h, or as long as

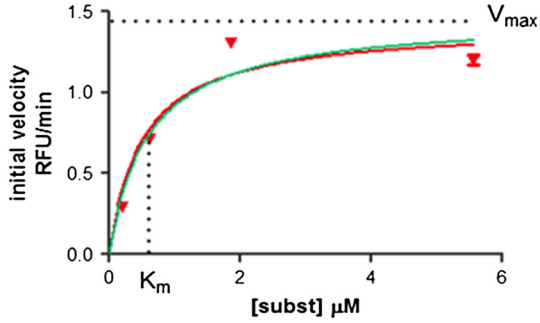

Figure 2. The plot of Michaelis–Menten type kinetics observed during the hydrolysis of the FRET substrate by HIV-1 PR, where V_{max} = 1.459 and K_m = 0.58 µM (red curve). The green curve represents the same data fit to the equation of a standard hyperbola.

Journal of PeptideScience

the data remained linear, at 1 min increments. The total reaction volume was 25 μl. All data presented are the average of at least duplicate measurements. The solubility of the tight binding inhibitor was sufficient for all the concentrations used. The DMSO/water mixture was used in a 1 : 9 ratio, and no precipitation was observed. Linear regression was performed on a plot of fractional velocity (v_i/v_o) *versus* inhibitor concentration to determine the total active site concentration (Figure 3). When the fractional velocity plateaus near zero, the enzyme is said to be completely, or nearly completely, inhibited and the rate of the reaction is determined simply by dissociation of the enzyme–inhibitor complex. The concentration of the tight binding inhibitor is said to be equal to the total active cite concentration, [E_t], at the *x*-intercept of the linear portion of the data, before the fractional velocity plateaus.

Inhibition assay

The K_i values were determined by a cell-free FRET-based assay using the FRET peptide substrate. Typically, 1 pmol (12 μl, 0.09 μM) of HIV-1 PR was added to 13 μl of dilution buffer A containing the substrate at a concentration near its K_m (1 μM) and various concentrations of the inhibitor dissolved in DMSO (final concentrations from 100 μM to 0.01 nM). The final concentrations of DMSO were kept below 2.5% (v/v). Substrate hydrolysis was followed as an increase in fluorescence (excitation/emission 490/530 nm). Data were collected at 25 °C for 1 h, or as long as the data remained linear, at 1 min increments. The total reaction volume was 25 μl. The solubility of the compounds was sufficient for all the concentrations used. The DMSO/water mixture was used in a 1 : 9 ratio, and no precipitation was observed. Inhibition data were analyzed using the equation for competitive inhibition according to Williams and Morrison [42]. The data were fit using nonlinear regression with the Graphpad Prism software [43].

Computational details

In this work, the crystal structure of HIV-1 PR complexed with a haloperidol derivative (pbd code, 1AID) was used [44]. The haloperidol derivative was removed from the structure; however, water molecules were kept for calculations. The system was submitted to a protein preparation process, which includes repairing of missing side-chain atoms, adding missing hydrogen atoms, assigning of amino acid atoms in biological pH (pH = 7) and finally restrained minimization. All of these approaches were performed using implemented protein preparation wizard in the Maestro program of the Schrodinger Suite [45]. Prior to docking simulation all the compounds used were assigned in physiological pH and geometry optimization was performed using LigPrep module of the Schrodinger Suite [46]. In order to perform theoretically reasonable binding affinity estimation, Induced Fir Docking (IFD) [47] protocol was employed; IFD has proven a useful method for the prediction of binding position and orientation of small molecules and particularly the estimation of their binding energies. It is possible to give flexibility to both ligand and receptor site with this program. The grid-docking box of the protein was identified utilizing the positions of Asp25 and Ile50 acid residues. IFD simulation includes three consequence steps as follows: (i) docking of ligands into the active site, (ii) refining of the amino acid atoms within 6 Å of the docked ligands, and (iii) re-docking of the ligand into the refined binding cavity. Finally, the ligand binding energy, which is obtained from the final docking, is considered as an IFD score.

Results and discussion

We have previously demonstrated that MD simulations can be a predictive method for the determination of the binding efficiency of fullerene amino acids in the binding pocket of HIV-1 PR (PDB code:1AID) [21]. During our preliminary studies we investigated the effects of the amino acid core and protecting groups. The most important observation was that the presence of the 9-fluorenylmethoxycarbonyl (Fmoc) protecting group on the [60]fullerene-substituted phenylalanine (i.e., Fmoc-Baa) improved the inhibition dramatically as compared with the corresponding free amine Baa (Figure 4a). Computation of the binding pose of Fmoc-Baa with HIV-1 PR showed that the large aromatic Fmoc group makes favorable interactions with the hydrophobic binding pocket [21]. Thus, we have maintained the Fmoc for the peptide derivatives.

All of our initial work has been with the [60]fullerene-substituted phenylalanine (Baa), unfortunately, the synthesis is lengthy (~2 weeks) and is low yield (~10%) [23]. Given that a threefold excess of the fullerene amino acid derivatives is required for solid phase ligation to a peptide sequence, we developed a simpler higher yield route involving the dipolar addition to C_{60} of the Fmoc-Nα-protected azido amino acids derived from phenylalanine,

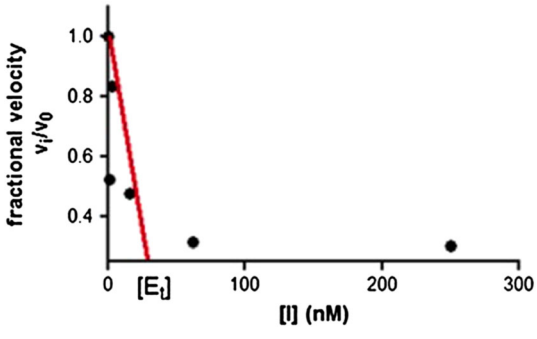

Figure 3. The plot of fractional velocity (v_i/v_o) *versus* inhibitor concentration used to determine the total active site concentration of the enzyme, [E_t] = 37.5 nM.

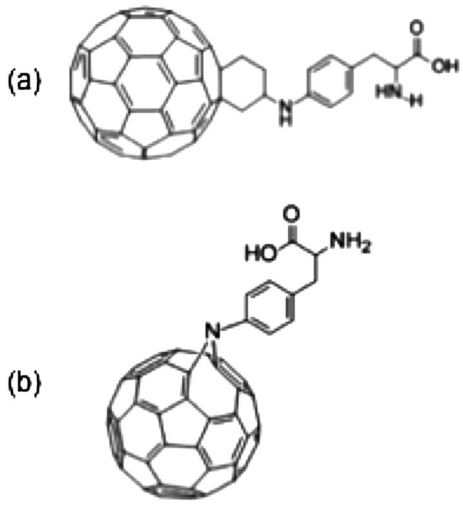

Figure 4. The chemical structures of (a) the [60]fullerene-substituted phenylalanine (Baa) and (b) the parent amino acid H-Phe(4-aza-C_{60})-OH. It should be noted that Baa is formed as a mixture of two diastereomers.

Figure 4b [25]. Thus, we have used Fmoc-Phe(4-aza-C_{60})-OH as the fullerene amino acid base for our peptide inhibitors because of its ease of preparation.

In choosing a series of model peptide sequences, we used Lipinski's rule of five for drug candidates as a guide in our inhibitor design [48,49]. The rule of five states that a drug lead should have no more than five H-bond donors, ten H-bond acceptors, a molecular weight under 500, and an octanol-water partition coefficient of 5 to be 'drug-like' and orally available. A tripeptide was determined to be the minimum length tail necessary to achieve these goals.

The rational for the design of three peptide models was based on the structure of HIV-1 PR itself. We hypothesized that an oligo-Lys peptide tail would provide both the positive charges and enough flexibility for the electrostatic interaction to occur [21]. In addition to the electrostatic interaction, the oligo-Lys tail should also improve the aqueous solubility of the C_{60} amino acid [24]. Even without the electrostatic interactions, at a minimum, the oligo-Lys tail should provide suitable H-bond donors and acceptors; thus, Fmoc-Phe(4-aza-C_{60})-Lys_3-OH (**1**) was chosen as the first model peptide (Figure 5). Finally, we used the knowledge that HIV-1 PR can recognize a Phe-Pro dipeptide subunit. Utilizing our C_{60} amino acid as the Phe component, the sequence Pro-Hyp-Lys was chosen with the second model peptide, i.e., Fmoc-Phe(4-aza-C_{60})-Pro-Hyp-Lys-OH (**2**). The final lysine residue was added both for aqueous solubility and to provide additional H-bonding opportunities with the binding pocket residues of HIV-1 PR. The final model, Fmoc-Phe(4-aza-C_{60})-Hyp-Hyp-Lys-OH (**3**) was chosen because the addition of the second OH group present on Hyp (as compared with Pro) allows another opportunity for H-bonding. In order to compare the effects of the fullerene (C_{60}) with a simple hydrophobic substituent and the Fmoc in the absence of the fullerene, stearic acid-Lys_3-OH (**4**) and Fmoc-Phe(4-NH_2)-Pro-Hyp-Lys-OH (**5**).were prepared. The structures of the peptides investigated as shown in Figure 5.

All C_{60} peptide inhibitors were made through SPPS. Fmoc-Phe(4-aza-C_{60})-OH was coupled to the peptide in the dark through standard Fmoc procedures. Because of the acid sensitivity of Fmoc-Phe(4-aza-C_{60})-OH, a solution of 20 : 2.5 : 77.5 TFA:TIPS:DCM was used to cleave the completed peptide sequence off the resin rather than the customary 95 : 2.5 : 2.5 TFA : TIPS:H_2O. The acidic cleavage from the SPPS resin results in a small degree of C_{60} loss and some conversion of the aza linkage to a primary amine. These were the minor impurities present by ESI/ToF MS in the peptide inhibitors post cleavage. The purity of the peptides cleaved from the resin was determined by HPLC with detection at 220 nm for the peptide and 330 nm for C_{60}. Figure 6 shows an HPLC chromatogram of Fmoc-Phe(4-aza-C_{60})-Lys_3-OH (**1**) illustrating their purity after cleavage from the resin. Based on ESI MS, the low retention time impurities are the amino peptide minus C_{60} and uncoupled peptide.

Because of the tendency of the C_{60} peptides to stick to any sort of column packing material, column purification was avoided when possible. Instead, peptide inhibitors were dissolved in DMSO at a concentration of ~500 μM and filtered through a C_{18} coated SiO_2 plug to remove any C_{60} present. The only impurity remaining was the amino peptide minus C_{60}, which has absorbance at 220 nm (peptide bond) and 256 nm (Phe residue). Therefore, the concentration of the C_{60} peptide inhibitors used in the assays was determined by UV at 330 nm (ε 0.0383 μM^{-1} cm^{-1}) to eliminate any absorption from amino peptide minus C_{60} (absorbance 256 nm).

The potency of an enzyme inhibitor is evaluated by monitoring the kinetics of the enzymatic reaction. This is accomplished by quantifying substrate depletion or product formation through chromogenic, radiometric, or HPLC based assays [50]. The values are usually given as EC_{50}, the dose required to affect a 50% decrease in the initial reaction velocity, or as K_i, the inhibition constant; both are reported in units of molarity. The inhibition constant is actually the dissociation constant of the enzyme/inhibitor complex and is considered to be a more accurate reflection of the pharmacokinetics of the inhibitor with the enzyme. In many cases the EC_{50} is roughly equivalent to the apparent K_i. However, in the case of tight binding inhibitors such as ours, the EC_{50} depends on the enzyme concentration and other conditions of the assay such as temperature and buffers. An inhibitor is considered to be tight binding when the inhibitor concentration used in the assay is near the total enzyme active site concentration, $[I] \approx [E_t]$. Because of their dependence on assay conditions, EC_{50} values are not always comparable to each other, whereas the inhibition constant, K_i, is a measure of the rate of dissociation of the complex and is therefore comparable to any other K_i measurement. In any case, the EC_{50} measurement is

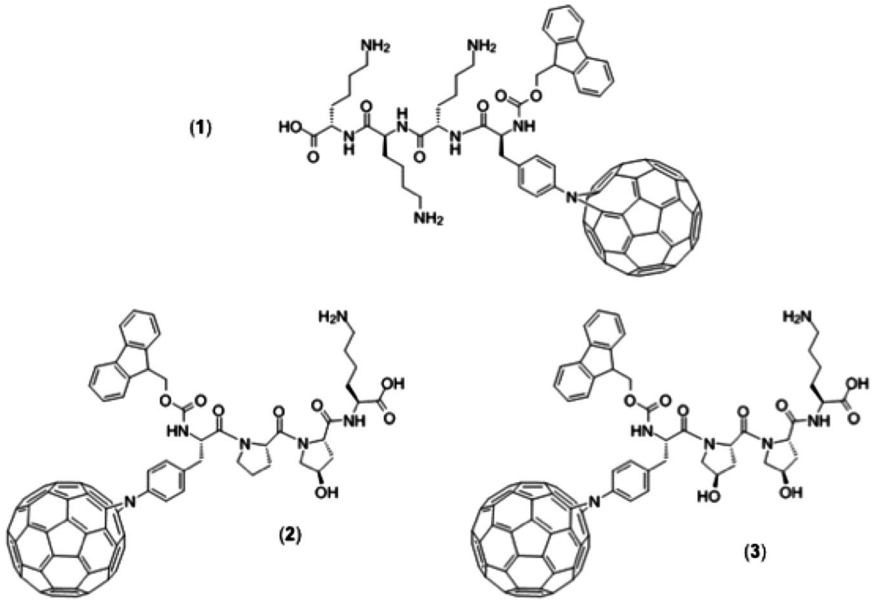

Figure 5. The chemical structure of the C_{60}-amino acid-based peptides synthesized and used in the present study.

Journal of PeptideScience

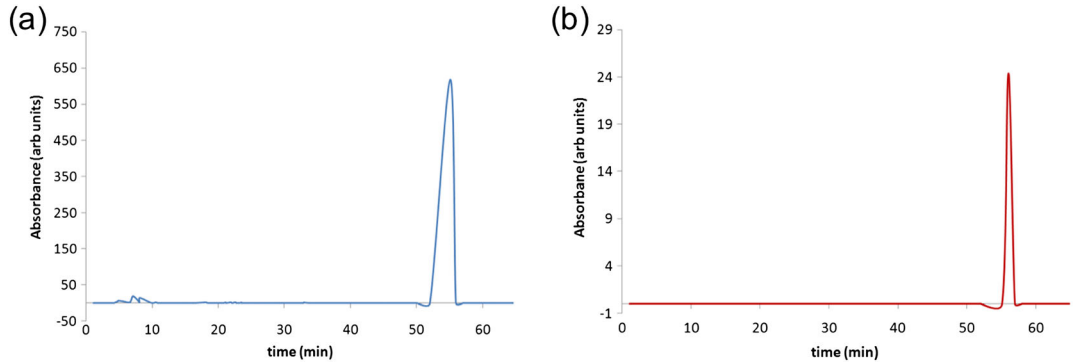

Figure 6. Typical HPLC chromatograms of Fmoc-Phe(4-aza-C_{60})-Lys_3-OH (**1**), with detection at (a) 220 nM for the peptide moieties and (b) 330 nm for the C_{60} moiety, illustrating the purity of the peptides after cleavage from the resin.

a less rigorous evaluation and is commonly used in high through put screening of inhibitors to determine lead compounds and can be converted to the K_i if other kinetic parameters of the substrate are known [41].

To determine the inhibition constant of our fullerene PRIs we utilized a FRET based assay to evaluate the enzyme kinetics of HIV-1 PR at various concentrations of inhibitors. To evaluate the K_m of our FRET substrate with HIV-1 PR we monitored the substrate hydrolysis at various substrate concentrations in the absence of inhibitors. The [E_t] was determined by titration with a tight-binding inhibitor. The K_m of our substrate was determined to be approximately 1 μM, and the [E_t] used in the assays was determined to be 37.5 nM. In addition to the kinetic constant K_m and the [E_t], a series of control experiments were also performed (Table 1).

The kinetic behavior of HIV-1 PR with our inhibitors was evaluated by a cell-free fluorescence resonance energy transfer (FRET) based assay using a FRET peptide substrate. FRET-based assays have become a popular method for high throughput screening of potential pharmacophores [51–53]. FRET is a distance-dependent interaction, and a FRET peptide consists of three main parts: a donor fluorophore (D), a quencher or acceptor molecule (A), and a linker between the two. When the donor is excited, its energy is transferred to the acceptor without the emission of a photon. Usually, the emission wavelength of the D moiety overlaps with the absorption wavelength of the acceptor. When the linker/peptide is cleaved the donor and acceptor are separated and the energy is no longer transferred resulting in a quantifiable fluorescence signal [54]. The FRET peptide used in our assay is derived from the native cleavage site on the polyprotein substrate of HIV-1 PR [54].

The inhibition constants of several amino acid PRIs as determined by cell-free FRET-based assay are given in Table 2 along with their simulated binding scores for comparison. The K_i for pepstatin A by this analysis method was 420 nM (literature value 500 nM) [55]. All of the C_{60} containing samples showed better inhibition than the non-C_{60} control by ~1000-fold. The hydrophobic control, Fmoc-Phe(4-NH_2)-OH, had in inhibition constant of >10 μM, in essence, no inhibition in comparison with any of the fullerene amino acids, which all exhibited at least nM inhibition. Inhibition constants of >10 μM are outside the determinable range by this analysis method. From this we can conclude that it is the presence of C_{60}, rather than it just being a hydrophobic entity, that is responsible for the observed inhibition. Both of the Fmoc protected amino acids [Fmoc-Baa, 36 nM, and Fmoc-Phe(4-aza-C_{60})-OH, 110 nM] showed improved inhibition over their free amine counterparts [Baa, 119 nM, and Phe(4-aza-C_{60})-OH, 120 nM] supporting our hypothesis that the Fmoc protecting group forms favorable interactions with the hydrophobic binding pocket. However, Fmoc-Phe(4-aza-C_{60})-OH was about three times less potent than the analogous Fmoc-Baa despite the fact that their deprotected analogs showed nearly equivalent inhibition, suggesting that the Baa linkage group offers an advantage presumably because of steric

Table 1. Control experiments performed before PRI analysis

Control	Description	Determination
Positive	no test compound	uninhibited reaction velocity, v_o
Inhibitor	pepstatin A	known inhibitor of HIV-1 PR
Vehicle	DMSO	inhibition because of vehicle
Test compound	assay buffer, no enzyme	autofluorescence of C_{60} PRIs
Substrate	assay buffer, no enzyme	baseline
C_{60} amino acid	Fmoc-Phe(4-NH_2)-OH	inhibition because of C_{60}
C_{60} peptide	Fmoc-Phe(4-NH_2)-Pro-Hyp-Lys-OH	inhibition because of C_{60}
Hydrophobic	Stearoyl-Lys_3-OH	inhibition because of hydrophobicity

Table 2. Inhibition constants of C_{60} amino acid PRIs, controls, and peptides

Compound	Inhibition constant, K_i (nM)	Experimental binding energy (kJ mol^{-1})	IFD score (kJ mol^{-1})
Pepstatin A	420	−36.3(3)	−37.1
Baa-OH	119	−39.7(1)	−39.5
Fmoc-Baa-OH	36	−42.8(1)	−42.7
Phe(4-aza-C_{60})-OH	120	−39.8(2)	−33.5
Fmoc-Phe(4-aza-C_{60})-OH	110	−39.7(2)	−39.7
Fmoc-Phe(4-aza-C_{60})-Lys_3-OH (**1**)	85	−40.3(1)	−40.0
Fmoc-Phe(4-aza-C_{60})-Pro-Hyp-Lys-OH (**2**)	120[a]	−40(2)	−38.1
Fmoc-Phe(4-aza-C_{60})-Hyp-Hyp-Lys-OH (**3**)	76	−40.6(2)	−40.1
Stearoyl-Lys_3-OH (**4**)	6310	−29.7(4)	−29.2
Fmoc-Phe-Pro-Hyp-Lys (**5**)	>10000	−23(1)	−33.8
Fmoc-Phe-OH	>10000	−25(1)	−26.2

[a]Indicates result from single data set.

differences (i.e., the distance between the amino acid groups and the C_{60}) [27]. Prediction of binding energy values of all used compounds was performed using IFD protocols as shown in Table 2. Our estimated binding energies are in a good quantitative agreement with experiments. Fmoc-Baa has shared the absolute highest binding affinity against HIV-1 as experimental result suggests. In the case of the c ontrol compounds (**4**, **5** and Fmoc-Phe-OH), estimated docking scores are small in absolute predicted binding affinity as compared with the fullerene bound compounds. These results are expected because of the fact that the fullerene could increase the inhibitory potential of compounds against HIV-1 protease.

The inhibition constant of the C_{60} peptides as determined by FRET based assays are given in Table 2 in addition to the simulated binding energies for comparison. As an example, Figure 7 shows the binding pose of Fmoc-Phe(4-aza-C_{60})-Lys_3-OH with HIV-1 PR as predicted by the IFD simulation. The most notable observation from the peptide experiments was that the predictive modeling program highly overestimated the inhibition of compound **5**, while the simple amino acid PRIs were well estimated. Although it may be argued that docking experiments can provide geometric analysis and characterization of a protein-peptide recognition event, but do not necessarily provide real information about the energetics of the process, we have previously shown an excellent correlation between experimental and computational data [21,31]. Given this prior relationship, a possible source of the discrepancy is that the peptide inhibitors are much more flexible and, particularly in the case of the Lys residues, have many possible conformations of the R side chains. In addition to the flexibility, the peptide inhibitors are much larger and possibly not well represented by the haloperidol crystal structure used in the MD simulations. In this regard, a crystal structure of HIV-1 PR with a peptide inhibitor, such as pepstatin A, may provide a more accurate starting point for the MD simulations of the larger peptide inhibitors.

In our investigation into the inhibition of HIV-1 PR with fullerene peptides we wanted to determine if just the presence of a hydrophobic moiety on a peptide sequence would have an effect on the observed inhibition of PR. In this regard, there was no suitable molecule that can mimic the hydrophobicity, size, and shape of C_{60}. Stearic acid has been shown to be membranotropic in much the same way as C_{60} because of its 18 carbon chain residue [56], and for that reason, it was chosen as a hydrophobic control. The SA-Lys_3-OH control showed inhibition of approximately 6.3 μM, better than other controls but still well below the potency of the C_{60} peptides. The inhibition constant of another non-C_{60} control peptide, Fmoc-Phe(4-NH_2)-Pro-Hyp-Lys-OH, was determined to be >10 μM, demonstrating again that the observed inhibition of the reaction velocity was because of C_{60} and not a result of the dipeptide recognition element, Phe-Pro.

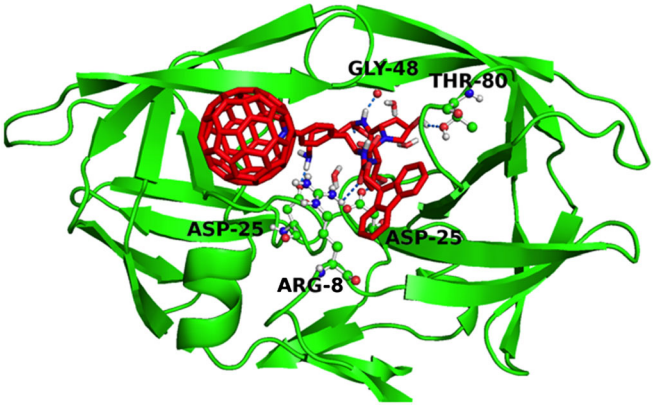

Figure 7. IFD position of Fmoc-Phe(4-aza-C_{60})-Lys_3-OH (**1**) into the active site. Dashed blue lines indicate H-bonds.

All of the peptide inhibitors showed improved inhibition over their C_{60} amino acid base; however, none were as effective as our most potent inhibitor, Fmoc-Baa-OH (K_i 36 nM). The most active of the peptide inhibitors was Fmoc-Phe(4-aza-C_{60})-Hyp-Hyp-Lys-OH (**3**) with two hydroxyproline residues (K_i = 76), which is much more active than Fmoc-Phe(4-aza-C_{60})-Pro-Hyp-Lys-OH (**2**) (K_i = 120), with only one hydroxyproline residue. It is unknown if the observed increase in binding affinity is because of better placement of the second hydroxyl moiety in regards to the aspartyl residues or if it is because of the increase in H-bonding opportunities; however the difference in energy is worth approximately that of a H-bond. Regardless, the Phe-Hyp dipeptide sequence does seem to be recognized by HIV-1 PR as we hypothesized. The oligo-Lys peptide, Fmoc-Phe(4-aza-C_{60})-Lys_3-OH (**1**), also showed improved inhibition over the C_{60} amino acid base. However, without a crystal structure it is impossible to determine if the positively charged Lys residues are forming a salt bridge or if the improved affinity is because of H-bonding. Calculation of the energy difference between Fmoc-Phe(4-aza-C_{60})-Lys_3-OH (**1**) and Fmoc-Phe(4-aza-C_{60})-OH reveals that a salt bridge, worth about 12–17 kJ mol^{-1}, is probably not the cause of the increase, which was approximately 0.6 kJ.mol^{-1}.

In comparison to currently marketed protease inhibitors, none of ours have yet achieved sub-nM levels of inhibition and therefore are not yet viable drug candidates. However, our results with both the amino acids and the peptides are encouraging indicators that the achieved inhibition may be tuned with minor alterations to both the peptide and amino acid structure. It should also be noted that almost all of our fullerene inhibitors show higher levels of inhibition in comparison with the most potent previously reported fullerene derivative (103 nM) [20].

Conclusions

Given that all of the peptide sequences studied improved the inhibition of the base fullerene amino acid, it is reasonable to assume that they will do the same for our other C_{60} amino acids. Since our most potent inhibitor was Fmoc-Baa, in future studies it should be used as the C_{60} amino acid base despite the length of time required for synthesis. However, we note that since Baa is a mixture of two diastereomers a future target should be to investigate the determination of individual inhibition constants.

In addition to the change in the amino acid base, in future studies the length of the peptides should be increased by one residue or more. Initially, when designing the peptides we used Lipinsky's rule of five for drug compounds as a guideline; however, a minimum sequence length was used for them all. However, HIV-1 PR recognizes peptides of at least five residues most efficiently [20]. We know that cationic fullerene peptide sequences cross a cellular membrane easily [26,29]; therefore, we surmise that we would not sacrifice membrane permeability by increasing the number of Lys residues on the tail and could potentially improve the molecular recognition with HIV-1 PR with the addition. Future work should maintain the Hyp_2 dipeptide subunit but should also include two or more Lys residue on the C-terminal end. This structural modification should improve solubility, make the peptide more recognizable by PR, and improve the affinity through H-bonding.

Journal of PeptideScience

Conflict of interests

The authors declare that there is no conflict of interests regarding the publication of this paper.

Acknowledgement

Financial support was provided by the Robert A. Welch Foundation (C-0002).

References

1 Davies DR. The structure and function of the aspartic proteinases. *Annu. Rev. Biophys. Biochem* 1990; **19**: 189–215.
2 Brik A, Wong C-H. HIV-1 protease: mechanism and drug discovery. *Org. Biomol. Chem.* 2003; **1**: 5–14.
3 Navia MA, Fitzgerald PMD, McKeever BM, Leu C-T, Heimbach JC, Herber WK, Sigal IS, Darke PL, Springer JP. Three-dimensional structure of aspartyl protease from human immunodeficiency virus HIV-1. *Nature* 1989; **337**: 615–620.
4 Kramer RA, Schaber MD, Skalka AM, Ganguly K, Wong-Staal F, Reddy EP. HTLV-III gag protein is processed in yeast cells by the virus pol-protease. *Science* 1986; **231**: 1580–1584.
5 Huff JR. HIV protease: a novel chemotherapeutic target for AIDS. *J. Med. Chem.* 1991; **34**: 2305–2314.
6 Babine RE, Bender SL. Molecular recognition of protein-ligand complexes: applications to drug design. *Chem. Rev.* 1997; **97**: 1359–1472.
7 Hyland LJ, Tomaszek TA, Meek TD. Human immunodeficiency virus-1 protease. 2. Use of pH rate studies and solvent kinetic isotope effects to elucidate details of chemical mechanism. *Biochemistry* 1991; **30**: 8454–8463.
8 James MNG (Ed). *Aspartic Proteinases: Retroviral and Cellular Enzymes*, Plenum Press: New York, 1998.
9 Suguna K, Padlan EA, Smith CW, Carlson WD, Davies DR. Binding of a reduced peptide inhibitor to the aspartic proteinase from Rhizopus chinensis: implications for a mechanism of action. *Proc. Natl. Acad. Sci. U. S. A.* 1987; **84**: 7009–7013.
10 Jaskólski M, Tomasselli AG, Sawyer TK, Staples DG, Heinrikson RL, Schneider J, Kent SBH, Wlodawer A. Structure at 2.5-.ANG. Resolution of chemically synthesized human immunodeficiency virus type 1 protease complexed with a hydroxyethylene-based inhibitor. *Biochemistry* 1991; **30**: 1600–1609.
11 Bernal JD, Crowfoot D. X-ray photographs of crystalline pepsin. *Nature* 1934; **133**: 794–795.
12 Wlodawer A, Vondrasek J. Inhibitors of HIV-1 protease: a major success of structure-assisted drug design. *Annu. Rev. Biophys. Biochem.* 1998; **27**: 249–284.
13 Aruksakunwong O, Promsri S, Wittayanarakul K, Nimmanpipug P, Lee VS, Wijitkosoom A, Sompornpisut P, Hannongbua S. Current development on HIV-1 protease inhibitors. *Curr. Comput.-Aid. Drug* 2007; **3**: 201–213.
14 Lefebvre E, Schiffer CA. Resilience to resistance of HIV-1 protease inhibitors: profile of Darunavir. *AIDS Rev.* 2008; **10**: 131–142.
15 Copeland RA. *Evaluation of Enzyme Inhibitors in Drug Discovery: A Guide for Medicinal Chemists and Pharmacologists*, Wiley: Hoboken, NJ, 2005.
16 Friedman SH, DeCamp DL, Sijbesma RP, Srdanov G, Wudl F, Kenyon GL. Inhibition of the HIV-1 protease by fullerene derivatives: model building studies and experimental verification. *J. Am. Chem. Soc.* 1993; **115**: 6506–6509.
17 Bosi S, Da Ros T, Spalluto G, Balzarini J, Prato M. Synthesis and anti-HIV properties of new water-soluble bis-functionalized[60]fullerene derivatives. *Bioorg. Med. Chem. Lett.* 2003; **13**: 4437–4440.
18 Schuster DI, Wilson LJ, Kirschner AN, Schinazi RF, Schlueter-Wirtz S, Tharnish P, Barnett T, Ermolieff J, Tang J, Brettreich M, Hirsch A. Evaluation of the anti-HIV potency of a water-soluble dendrimeric fullerene. *Electrochem. Soc. Proc.* 2000; **11**: 267–270.
19 Marchesan S, Da Ros T, Spalluto G, Balzarini J, Prato M. Anti-HIV properties of cationic fullerene derivatives. *Bioorg. Med. Chem. Lett.* 2005; **15**: 3615–3618.
20 Friedman SH, Ganapathi PS, Rubin Y, Kenyon GL. Optimizing the binding of fullerene inhibitors of the HIV-1 protease through predicted increases in hydrophobic desolvation. *J. Med. Chem.* 1998; **41**: 2424–2429.
21 Durdagi S, Supuran CT, Strom TA, Doostdar N, Kumar MK, Barron AR, Mavromoustakos T, Papadopoulos MG. In silico drug screening approach to designing magic bullets: a successful example with anti-HIV fullerene derivatized amino acids. *J. Chem. Inf. Model.* 2009; **49**: 1139–1143.
22 Prato M, Bianco A, Maggini M, Scorrano G, Toniolo C, Wudl F. Synthesis and characterization of the first fullerene-peptide. *J. Org. Chem.* 1993; **58**: 5578–5580.
23 Yang J, Barron AR. A new route to fullerene substituted phenylalanine derivatives. *Chem. Commun.* 2004; **40**: 2884–2885.
24 Yang J, Alemany LB, Driver J, Hartgerink JD, Barron AR. Fullerene-derivatized amino acids: synthesis, characterization, antioxidant properties, and solid phase peptide synthesis. *Chem. Eur. J.* 2007; **13**: 2530–2545.
25 Strom TA, Barron AR. A simple quick route to fullerene amino acid derivatives. *Chem. Commun.* 2010; **46**: 4764–4766.
26 Yang J, Wang K, Driver J, Yang J, Barron AR. The use of fullerene substituted phenylalanine derivatives as a passport through cell membranes. *Org. Biomol. Chem.* 2007; **5**: 260–266.
27 Strom TA, Barron AR. Attempts towards the Bucky-amino acid acylation of the phospho-cytidine-phospho-adenosine (pdCpA) subunit. *All Res. J. Nano* 2015; **1**: 4–9.
28 Rouse JG, Yang J, Barron AR, Monteiro-Riviere NA. Fullerene-based amino acid interactions with human epidermal keratinocytes. *Toxicol. In Vitro* 2006; **8**: 1313–1320.
29 Zhang LW, Yang J, Barron AR, Monteiro-Riviere NA. Endocytic mechanisms and toxicity of a functionalized fullerene in human cells. *Toxicol. Lett.* 2009; **191**: 149–157.
30 Rouse JG, Ryman-Rasmussen JP, Yang J, Barron AR, Monteiro-Riviere NA. Effects of mechanical flexion on the penetration of fullerene amino acid-derivatized peptide nanoparticles through skin. *Nano Lett.* 2007; **7**: 155–160.
31 Innocenti A, Durdagi S, Doostdar N, Strom TA, Barron AR, Supuran CT. Nanoscale enzyme inhibitors: fullerenes inhibit carbonic anhydrase by occluding the active site entrance. *Bioorg. Med. Chem.* 2010; **18**: 2822–2828.
32 Andreeva I, Petrukhina A, Garmanova A, Babakhin A, Andreev S, Romanova V, Troshin P, Troshina O, DuBuske L. Penetration of fullerene C_{60} derivatives through biological membranes. *Fuller. Nanotub. Car. N.* 2008; **16**: 89–102.
33 Pellarini F, Pantarotto D, Da Ros T, Giangaspero A, Tossi A, Prato M. A Novel [60]fullerene amino acid for use in solid-phase peptide synthesis. *Org. Lett.* 2001; **3**: 1845–1848.
34 Bianco A, Da Ros T, Prato M, Toniolo C. Fullerene-based amino acids and peptides. *J. Pept. Sci.* 2001; **7**: 208–219.
35 Pantarotto D, Tagmatarchis N, Bianco A, Prato M. Synthesis and biological properties of fullerene-containing amino acids and peptides. *Mini-Rev. Med. Chem.* 2004; **4**: 805–814.
36 Kobzar OL, Trush VV, Tanchuk VY, Zhilenkov AV, Troshin PA, Vovk AI. Fullerene derivatives as a new class of inhibitors of protein tyrosine phosphatases. *Bioorg. Med. Chem. Lett.* 2014; **24**: 3175–3179.
37 Zanzoni S, Ceccon A, Assfalg M, Singh RK, Fushman D, D'Onofrio M. Polyhydroxylated [60]fullerene binds specifically to functional recognition sites on a monomeric and a dimeric ubiquitin. *Nanoscale* 2015; **7**: 7197–7205.
38 Pang X, Liu Z, Zhai G. Advances in non-peptidomimetic HIV protease inhibitors. *Curr. Med. Chem.* 2014; **21**: 1997–2011.
39 Durdagi S, Mavromoustakos T, Chronakis N, Papadopoulos MG. Computational design of novel fullerene analogs as potential HIV 1 PR inhibitors: analysis of the binding interactions between fullerene inhibitors and HIV 1 PR residues using 3D QSAR, molecular docking and molecular dynamics simulations. *Bioorg. Med. Chem.* 2008; **16**: 9957–9974.
40 NovaBiochem Catalog & Peptide Synthesis Handbook, 1999, NovaBiochem, La Jolla, California.
41 Marangoni AG. *Enzyme Kinetics: A Modern Approach*, Wiley: Hoboken, New Jersey, 2003.
42 Williams JW, Morrison JF. The kinetics of reversible tight-binding inhibition. *Methods Enzymol.* 1979; **63**: 437–467.
43 Non-linear regression determination of Morrison Ki performed on GraphPad Prism version 5.03 for Windows, GraphPad Software, San Diego California USA, www.graphpad.com. nd
44 Rutenber W, Fauman EB, Keenan RJ, Fong S, Furth PS, Ortiz de Montellano PR, Meng E, Kuntz ID, DeCamp DL, Salto R, Rosb JR, Craik CS, Stroud RM. Structure of a non-peptide inhibitor complexed with HIV-1 protease. Developing a cycle of structure-based drug design. *J. Biol. Chem.* 1993; **268**: 15343–15346.

45 Madhavi Sastry G, Adzhigirey M, Day T, Annabhimoju R, Sherman W. Protein and ligand preparation: parameters, protocols, and influence on virtual screening enrichments. *J. Comput. Aided Mol. Des.* 2013; **27**: 221–234.
46 Schrödinger Release 2015–2: LigPrep, version 3.4, Schrödinger, LLC, New York, NY, 2015
47 Farid R, Day T, Friesner RA, Pearlstein RA. New insights about HERG blockade obtained from protein modeling, potential energy mapping, and docking studies. *Bioorg. Med. Chem.* 2006; **14**: 3160–3173.
48 Lipinski CA. Lead- and drug-like compounds: the rule-of-five revolution. *Drug Discov. Today* 2004; **1**: 337–341.
49 Lipinski CA. Drug-like properties and the causes of poor solubility and poor permeability. *J. Pharmacol. Toxicol.* 2000; **44**: 235–249.
50 Copeland RA. *Evaluation of Enzyme Inhibitors in Drug Discovery: A Guide for Medicinal Chemists and Pharmacologists*, Wiley: Hoboken, NJ, 2005.
51 Rodems SM, Hamman BD, Lin C, Zhao J, Shah S, Heidary D, Makings L, Stack JH, Pollok BA. A FRET-based assay platform for ultra-high density drug screening of protein kinases and phosphatases. *Assay Drug Dev. Technol.* 2002; **1**: 9–19.
52 Liu Y-C, Huang V, Chao T-C, Hsiao C-D, Lin A, Chang M-F, Chow L-P. Screening of drugs by FRET analysis identifies inhibitors of SARS-CoV 3CL protease. *Biochem. Biophys. Res. Co.* 2005; **333**: 194–199.
53 Zaman GJR, Garritsen A, de Boer T van Boeckel CAA. Fluorescence assays for high-throughput screening of protein kinases. *Comb. Chem. High Technol Scr.* 2003; **6**: 313–320.
54 User Manual for Pro-AssayTM HIV-1 Protease Assay Kit from ProteinOne. nd
55 Furfine ES. HIV protease assays. *Curr. Protocols Pharmacol.* 2001; **00**: 3.2.1–3.2.12.
56 Trabulo S, Cardoso AL, Mano M, Pedroso de Lima MC. Cell-penetrating peptides-mechanisms of cellular uptake and generation of delivery systems. *Pharmaceuticals* 2010; **3**: 961–993.

